J. Braz. Chem. Soc., Vol. 19, No. 3, 426-433, 2008.
Printed in Brazil - ©2008 Sociedade Brasileira de Química
0103 - 5053 $6.00+0.00

Article

Preparation, Cation-Anion Interactions and Physicochemical Properties of Ether-Functionalized Imidazolium Ionic Liquids

Henri S. Schrekker,* Dagoberto O. Silva, Marcos A. Gelesky, Marcelo P. Stracke, Clarissa M. L. Schrekker, Reinaldo S. Gonçalves and Jairton Dupont*

Instituto de Química, Universidade Federal do Rio Grande do Sul, Av. Bento Gonçalves, 9500, CP 15003, 91501-970 Porto Alegre-RS, Brazil

Uma série de líquidos iônicos 1-alquil éter (e 1-alquil)-3-metilimidazólio **2**-**4** ($[C_xO_yMIm]^+[Ânion]^-$ ou $[C_xMIm]^+[Ânion]^-$, onde MIm = 3-metilimidazólio; C_xO_y = 1-alquil éter, C_7O_3 = $-(CH_2)_2O(CH_2)_2O(CH_2)_2OCH_3$ (**A**), C_3O_1 = $-(CH_2)_2OCH_3$ (**B**); C_x = 1-alquil, C_{10} = $C_{10}H_{21}$ (**C**), C_4 = C_4H_9 (**D**); e $[Ânion]^-$ = $H_3CSO_3^-$ (**2**), BF_4^- (**3**) ou PF_6^- (**4**)) foram preparados e caracterizados. A força da ligação de hidrogênio entre o cátion e o ânion dos líquidos iônicos **2**-**4** depende principalmente do ânion e diminui na ordem $H_3CSO_3^- > BF_4^- > PF_6^-$. Todos os líquidos iônicos metanosulfonatos **2** possuem uma forte desblindagem para o próton H^2 do ciclo imidazólio. Os líquidos iônicos funcionalizados com um grupo 1-alquil éter mostram densidades mais altas em comparação com seus equivalentes do grupo 1-alquil. Os sais **2a**-**b**, **3a**-**d** e **4a**-**b** são líquidos iônicos à temperatura ambiente. E, todos os líquidos iônicos 1-alquil éter funcionalizados (exceto **4b**) são completamente amorfos. As maiores faixas líquidas foram obtidas com os líquidos iônicos tetrafluoroborato devido as suas solidificações a temperaturas baixas e excelente estabilidade térmica. Estes dados fornecem informações importantes para o entendimento sobre possíveis aplicações e a preparação de líquidos iônicos com tarefas específicas.

A set of 1-alkyl ether (and 1-alkyl)-3-methylimidazolium ionic liquids **2**-**4** ($[C_xO_yMIm]^+[Anion]^-$ or $[C_xMIm]^+[Anion]^-$, where MIm = 3-methylimidazolium; C_xO_y = 1-alkyl ether, C_7O_3 = $-(CH_2)_2O(CH_2)_2O(CH_2)_2OCH_3$ (**A**), C_3O_1 = $-(CH_2)_2OCH_3$ (**B**); C_x = 1-alkyl, C_{10} = $C_{10}H_{21}$ (**C**), C_4 = C_4H_9 (**D**); and $[Anion]^-$ = $H_3CSO_3^-$ (**2**), BF_4^- (**3**) or PF_6^- (**4**)) was prepared and characterized. The cation-anion hydrogen bonding strength showed to be mainly anion dependent and decreased in the order $H_3CSO_3^- > BF_4^- > PF_6^-$. All methanesulfonate ionic liquids **2** possessed a strongly deshielded H^2 imidazolium ring proton. 1-Alkyl ether functionalized ionic liquids showed higher densities in comparison to their 1-alkyl equivalents. The salts **2a**-**b**, **3a**-**d** and **4a**-**b** are room-temperature ionic liquids. All 1-alkyl ether functionalized ionic liquids (except **4b**) are completely amorphous. The widest liquid ranges were obtained with the tetrafluoroborate ionic liquids due to their late solidification and excellent thermal stability. These data provide important information for the understanding of their application scope and the preparation of task-specific ionic liquids.

Keywords: imidazolium ionic liquids, ether-functionalized, hydrogen bonding, physicochemical properties, task-specific

Introduction

Room-temperature ionic liquids (RTILs), ionic salts that melt at and below ambient temperature, typically comprise of an organic cation and an organic or inorganic anion. The class of imidazolium RTILs is used in a wide variety of applications due to their attractive physical and chemical properties,[1-3] which include: air and moisture stability, low flammability, thermal stability, a neglectable vapor pressure, being liquid over a wide temperature range, wide electrochemical windows, high conductivities and ionic mobilities, easy recycling, tunable miscibility

*e-mail: schrekker@iq.ufrgs.br; dupont@iq.ufrgs.br

with water and organic solvents, and being a good solvent for a wide variety of organic and inorganic chemical compounds. As a result, imidazolium RTILs are applied in, for instance, synthetic chemistry,[1,3] (biphasic) catalysis,[2-4] extraction/separation processes,[1] material science[1,5] and electrochemistry.[6] The number of imidazolium RTIL applications is expanding rapidly as structural modifications are easily introduced in both the imidazolium cation (especially the 1 and 3 positions of the imidazolium ring) and the anion, which promotes the development of task-specific RTILs.[7] As part of our research program we pursued the application of ether-functionalized imidazolium RTILs (Figure 1, cations **A** and **B**).[8]

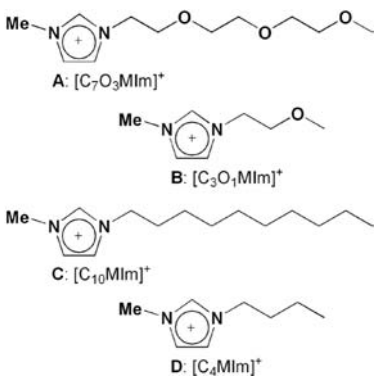

Figure 1. 1-Alkyl ether (and 1-alkyl)-3-methylimidazolium cations **A-D**.

The preparation and characterization of a variety of ether-functionalized imidazolium RTILs are reported in the literature.[9-12] Applications of these are found in the fields of molecular-recognition,[13] transition-metal catalysis,[14] biocatalysis,[15] carbohydrate/nucleoside chemistry,[16,17] anti-microbial activities,[18] metal extraction,[19] liquid-phase organic synthesis,[20] polymer chemistry,[21] organic synthesis,[22] self-organization[23] and lubricants.[24] Understanding how structural changes affect physicochemical properties is of great importance for the preparation of task-specific RTILs. We report herein the synthesis, cation-anion interactions and physicochemical properties of a complementary set of 1-alkyl ether (and 1-alkyl)-3-methylimidazolium ILs **2**-**4** (Figure 2).

Experimental

Density

The densities of **2a**-**b**, **3a**-**c** and **4a**-**b** were determined by measuring the weight of 5.0 mL IL at a constant temperature of 30 °C. A volumetric flask was calibrated with distilled water at 30 °C using a density of 0.995646 g mL^{-1} for water.[25]

Differential Scanning Calorimetry (DSC)

The phase transitions of **2a**-**d**, **3a**-**d** and **4a**-**b** were determined using a TA Instruments DSC 2010 differential scanning calorimeter, equipped with a manual cooling unit. The DSC instrument was calibrated using indium. An average sample weight of 10-20 mg was sealed in an aluminium pan. RTILs were cooled to –100 °C, heated to 70 °C, cooled to –100 °C and heated to 70 °C at a rate of 10 °C min^{-1} under a flow of nitrogen. Room-temperature ionic solids were heated to 100 °C, cooled to –100 °C and heated to 100 °C at a rate of 10 °C min^{-1} under a flow of nitrogen. The glass transition temperature (T_g, determined at the onset of the heat capacity change), crystallization temperature (T_c, determined at the onset of the exothermic peak), and melting point (T_m, determined at the onset of the endothermic peak) were determined on heating in the second heating run.

Thermal Gravimetric Analysis (TGA)

TGA measurements of **2a**-**c**, **3a**-**c** and **4a**-**b** were performed on a TA Instruments Q50 thermogravimetric analyzer. The TGA instrument was calibrated using nickel. An average sample weight of 8-12 mg was placed in a

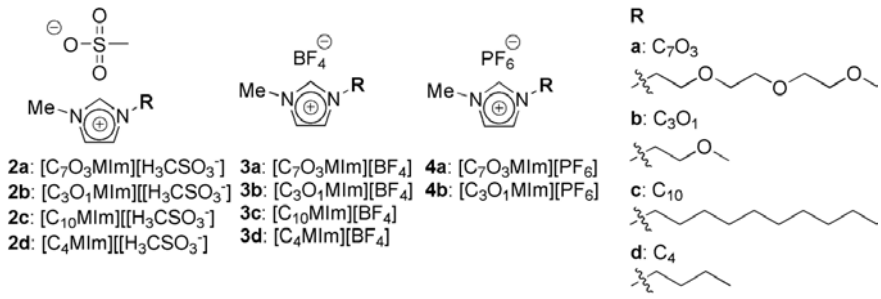

Figure 2. Imidazolium ILs prepared and studied in this work.

platinum pan and heated at 20 °C min^{-1} from ca. 30 to 800 °C under a flow of nitrogen. The onset of decomposition was defined as the decomposition temperature (T_d).

*Triethylene glycol monomethyl ether methanesulfonate (**1a**)*

Triethylene glycol monomethyl ether (125 mL, 798 mmol, 1.00 equiv.), methanesulfonyl chloride (65 mL, 838 mmol, 1.05 equiv.), triethylamine (122 mL, 878 mmol, 1.10 equiv.) and dichloromethane (700 mL). Alkylating agent **1a** was isolated in a yield of 95 %. ^{1}H NMR (300 MHz, $CDCl_3$, 298 K) δ 4.39 (m, 2H), 3.77 (m, 2H), 3.71-3.61 (m, 6H), 3.57-3.52 (m, 2H), 3.38 (s, 3H), 3.08 (s, 3H); ^{13}C{^{1}H} NMR (75.4 MHz, $CDCl_3$, 298 K) δ 71.2 (CH_2), 69.9 (CH_2), 69.8 (CH_2), 69.7 (CH_2), 69.0 (CH_2), 68.3 (CH_2), 58.3 (CH_3), 36.9 (CH_3); IR (neat) ν_{max}/cm^{-1}: 3019 (w), 2934 (w), 2880 (s), 1454 (m), 1414 (w), 1351 (s), 1301 (m), 1248 (m), 1199 (m), 1175 (s), 1131 (s), 1106 (s), 1017 (s), 975 (s), 922 (s), 850 (m), 809 (m), 733 (w), 529 (s); MS-ESI+ *m*/*z* (%): $C_8H_{19}O_6S$ $[M+H]^+$ 243.2 (100).

*1-Triethylene glycol monomethyl ether-3-methylimidazolium methanesulfonate (**2a**)*

^{1}H NMR (300.0 MHz, $CDCl_3$, 298 K) δ 9.62 (bs, 1H), 7.66 (bs, 1H), 7.47 (bs, 1H), 4.54 (t, *J* 4.7, 2H), 4.02 (s, 3H), 3.88 (t, *J* 4.7, 2H), 3.67-3.60 (m, 6H), 3.57-3.53(m, 2H), 3.38 (s, 3H), 2.85 (s, 3H); ^{13}C{^{1}H} NMR (75.4 MHz, $CDCl_3$, 298 K) δ 137.6 (CH), 123.2 (CH), 122.8 (CH), 71.5 (CH_2), 70.0 (CH_2), 69.9 (CH_2), 69.8 (CH_2), 68.7 (CH_2), 58.6 (CH_3), 49.2 (CH_2), 39.4 (CH_3), 35.9 (CH_3); IR (neat) ν_{max}/cm^{-1}: 3147 (w), 3096 (m), 3006 (w), 2930 (m), 2876 (m), 2834 (w), 2747 (w), 1573 (m), 1456 (m), 1430 (w), 1351 (m), 1329 (w), 1289 (m), 1211 (s), 1200 (s), 1107 (s), 1040 (s), 964 (w), 934 (w), 850 (m), 767 (m), 655 (w), 625 (w), 552 (m), 526 (m); MS-ESI+ *m*/*z* (%): $C_{11}H_{21}N_2O_3$ $[M-CH_3O_3S]^+$ 229.2 (100), $C_{23}H_{45}N_4O_9S$ $[M+C_{11}H_{21}N_2O_3]^+$ 553.4 (0.09).

*1-Decyl-3-methylimidazolium methanesulfonate (**2c**)*

^{1}H NMR (300.0 MHz, $CDCl_3$, 298 K) δ 9.83 (bs, 1H), 7.51 (bs, 1H), 7.36 (bs, 1H), 4.25 (t, *J* 7.4, 2H), 4.05 (s, 3H), 2.79 (s, 3H), 1.88 (m, 2H), 1.32-1.25 (m, 14H), 0.88 (t, *J* 6.7, 3H); ^{13}C{^{1}H} NMR (75.4 MHz, $CDCl_3$, 298 K) δ 137.1 (CH), 123.4 (CH), 121.7 (CH), 49.3 (CH_2), 39.2 (CH_3), 35.7 (CH_3), 31.2 (CH_2), 29.7 (CH_2), 28.9 (CH_2), 28.8 (CH_2), 28.7 (CH_2), 28.4 (CH_2), 25.7 (CH_2), 22.1 (CH_2), 13.6 (CH_3); IR (film) ν_{max}/cm^{-1}: 3147 (w), 3092 (w), 3053 (w), 3017 (w), 2956 (w), 2926 (m), 2855 (w), 1573 (w), 1467 (w), 1265 (w), 1239 (w), 1206 (s), 1193 (s), 1058 (m), 784 (w), 772 (w), 734 (m), 701 (w), 624 (w), 562 (w), 536 (w), 526 (w); MS-ESI+ *m*/*z* (%): $C_{14}H_{27}N_2$ $[M-CH_3O_3S]^+$ 223.2 (100), $C_{29}H_{57}N_4O_3S$ $[M+C_{14}H_{27}N_2]^+$ 541.5 (0.05).

*1-Triethylene glycol monomethyl ether-3-methylimidazolium tetrafluoroborate (**3a**)*

^{1}H NMR (300.0 MHz, d6-acetone, 298 K) δ 9.00 (bs, 1H), 7.77 (bs, 1H), 7.68 (bs, 1H), 4.52 (t, *J* 4.8, 2H), 4.07 (s, 3H), 3.92 (t, *J* 4.8, 2H), 3.68-3.48 (m, 8H), 3.31 (s, 3H); ^{13}C{^{1}H} NMR (75.4 MHz, d6-acetone, 298 K) δ 138.5 (CH), 124.8 (CH), 124.5 (CH), 73.1 (CH_2), 71.4 (2xCH_2), 71.3 (CH_2), 69.9 (CH_2), 59.3 (CH_3), 50.7 (CH_2), 37.0 (CH_3); IR (neat) ν_{max}/cm^{-1}: 3158 (w), 3118 (w), 2930 (w), 2880 (w), 2824 (w), 2743 (w), 1575 (w), 1455 (w), 1352 (w), 1286 (w), 1245 (w), 1199 (w), 1172 (m), 1059 (s), 850 (w), 624 (w), 521 (w); MS-ESI+ *m*/*z* (%): $C_{11}H_{21}N_2O_3$ $[M-BF_4]^+$ 229.2 (100), $C_{22}H_{42}BF_4N_4O_6$ $[M+C_{11}H_{21}N_2O_3]^+$ 545.4 (0.2).

*1-Triethylene glycol monomethyl ether-3-methylimidazolium hexafluorophosphate (**4a**)*

^{1}H NMR (300.0 MHz, d6-acetone, 298 K) δ 9.02 (bs, 1H), 7.78 (bs, 1H), 7.69 (bs, 1H), 4.53 (t, *J* 4.8, 2H), 4.08 (s, 3H), 3.92 (m, 2H), 3.68-3.49 (m, 8H), 3.30 (s, 3H); ^{13}C{^{1}H} NMR (75.4 MHz, d6-acetone, 298 K) δ 138.5 (CH), 124.8 (CH), 124.6 (CH), 73.1 (CH_2), 71.5 (3xCH_2), 69.9 (CH_2), 59.3 (CH_3), 51.0 (CH_2), 37.1 (CH_3); IR (neat) ν_{max}/cm^{-1}: 3166 (m), 3122 (m), 3084 (m), 2929 (m), 2882 (m), 2829 (m), 2748 (w), 1576 (m), 1456 (m), 1431 (w), 1387 (w), 1352 (m), 1295 (w), 1249 (w), 1199 (m), 1171 (s) 1104 (s), 1041 (m), 1027 (m), 934 (w), 853 (s), 842 (s), 776 (w), 752 (m), 741 (w), 653 (m), 624 (m), 559 (s); MS-ESI+ *m*/*z* (%): $C_{11}H_{21}N_2O_3$ $[M-PF_6]^+$ 229.1 (100), $C_{22}H_{42}F_6N_4O_6P$ $[M+C_{11}H_{21}N_2O_3]^+$ 603.3 (0.6).

Results and Discussion

Synthesis

A straightforward synthetic sequence (Scheme 1) was chosen for the preparation of halide-free imidazolium ILs **2-4** (Figure 2).[11] The methanesulfonate ester alkylating agents **1** are easily accessible by the treatment of the corresponding alcohols with methanesulfonyl chloride in the presence of triethylamine. In contrast to the lower molecular weight methanesulfonate esters **1b** and **1d**, **1a** and **1c** decomposed at elevated temperatures before distillation started. A treatment with activated carbon completely removed the small quantity of yellow impurities from **1c**, but not from **1a**. All methanesulfonate esters **1** were isolated in high yields (> 90%).

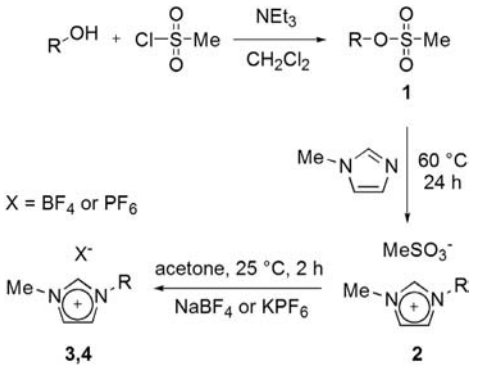

Scheme 1. General synthetic route for the synthesis of the imidazolium ILs **2-4**.

The alkylations of 1-methylimidazole with the methanesulfonate esters **1** were performed under solventless conditions at 60 °C for 24 hours (Scheme 1). Room-temperature ionic solids were obtained in the reactions with the alkyl methanesulfonate esters **1c** and **1d**, which allowed a facile re-crystallization for the purification of **2c** and **2d**. The 1-alkyl-3-methylimidazolium methanesulfonate salts **2c** and **2d** were obtained as ultra pure and white crystals in high yields (>90 %). In contrast, the 1-alkyl ether-3-methylimidazolium methanesulfonate salts **2a** and **2b** are RTILs and re-crystallization attempts were unsuccessful for both. An acid-base purification procedure with methanesulfonic acid was applied as alternative to remove the slight excess of 1-methylimidazole. According to NMR spectral data, RTILs **2a** and **2b** were isolated as analytical pure yellow liquids in yields of > 90% after an activated carbon treatment. Undoubtly, re-crystallization was the only suitable purification procedure for the removal of the small quantities of yellow impurities. All methanesulfonate ILs **2** are extremely hygroscopic.

Preparation of the tetrafluoroborate **3** and hexafluoro-phosphate **4** ILs in high yields of > 90% was achieved by an anion metathesis of **2** in the presence of either $NaBF_4$ or KPF_6 at room-temperature for 2 hours.[9] The 1-alkyl RTILs **3c** and **3d** were isolated as colorless liquids and the 1-alkyl ether RTILs **3a**-**b** and **4a**-**b** were obtained as yellow liquids.

This complementary set of ILs **2**-**4** made it possible to study the correlation between structural modifications and physicochemical properties: (*i*) Imidazolium cations – Comparison of the 1-alkyl ether functional groups with the 1-alkyl chains due to the same number of atoms (C_7O_3 **a** *versus* C_{10} **c** and C_3O_1 **b** *versus* C_4 **d**); (*ii*) Imidazolium cations – Comparison of the length of the 1-alkyl ether and 1-alkyl chains (C_7O_3 **a** *versus* C_3O_1 **b** and C_{10} **c** *versus* C_4 **d**); (*iii*) IL anions – Comparison of methanesulfonate **2** *versus* tetrafluoroborate **3** *versus* hexafluorophosphate **4**. ^{1}H NMR, ^{13}C NMR, IR, MS-ESI, DSC, TGA and density measurements were performed for the characterization of the ILs **2-4**, and to study the imidazolium cation-anion interactions and physicochemical properties.

Hydrogen bonding strength

Imidazolium ILs exist as hydrogen-bonded networks in both solid and liquid phases.[26-28] Each imidazolium cation is surrounded by anions and each anion is surrounded by imidazolium cations in an extended network due to the formation of hydrogen bonds between the imidazolium ring protons and anions. It is especially this feature what distinguishes the imidazolium ILs from other types of ILs that form neutral ion pairs. Knowledge of the hydrogen bonding strengths could result in a better understanding of the correlation between structural modifications and physicochemical properties. An infrared spectroscopy study of the ILs **2**-**4** was performed to obtain information about the inter-ionic hydrogen bonding interactions.[28-30] The imidazolium ring proton numbers used in this work are shown in Figure 3.

The IR spectral data of the aromatic C-H stretching region between 3200 and 3000 cm^{-1} are presented in Table 1.

Table 1. Infrared spectral data for the aromatic stretching region (3200-3000 cm^{-1}), corresponding with C-H stretching frequencies of the imidazolium cation

2-4	Cation	Anion	ν [C-H^5]	ν [C-H^4]	ν [C-H^2]
2a	$[C_7O_3MIm]^+$	$[H_3CSO_3]^-$	3147	3096	3006
2b	$[C_3O_1MIm]^+$	$[H_3CSO_3]^-$	3147	3096	3006
2c	$[C_{10}MIm]^+$	$[H_3CSO_3]^-$	3147	3092[a]	3017[a]
3a	$[C_7O_3MIm]^+$	$[BF_4]^-$	3158	3118	n.o.[b]
3b	$[C_3O_1MIm]^+$	$[BF_4]^-$	3164	3123	n.o.[b]
3c	$[C_{10}MIm]^+$	$[BF_4]^-$	3162	3122	n.o.[b]
4a	$[C_7O_3MIm]^+$	$[PF_6]^-$	3166	3121	3084
4b	$[C_3O_1MIm]^+$	$[PF_6]^-$	3171	3125	n.o.[b]

[a]Additional stretching frequency observed at 3053 cm^{-1}. [b]Not observed.

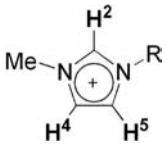

Figure 3. Imidazolium ring proton numbers.

Three characteristic infrared bands (ν [C-H^5], ν [C-H^4] and ν [C-H^2]) are expected in this region for the aromatic C-H stretching vibrations in the imidazolium ring.

Methanesulfonate RTIL **2a** showed three stretching frequencies at 3147, 3096 and 3006 cm^{-1}, respectively. A shift to lower frequencies, corresponding to a reduced strength of the aromatic C-H bond, is the consequence of an increased hydrogen bonding participation.[28,29] The value of 3006 cm^{-1} for ν [C-H^2] corresponds to a very strong hydrogen bonding interaction. Theoretical calculations show that the H^2 proton bears the largest positive charge of the aromatic imidazolium protons and is, therefore, the strongest hydrogen bond donor.[30,31] The hydrogen bonding strengths are mainly anion dependent and decrease in the order $H_3CSO_3^- > BF_4^- > PF_6^-$. Noticeable is the drastically reduced hydrogen bond interaction between the PF_6^- anion and H^2 proton of RTIL **4a**. The influence of the 1-alkyl ether and 1-alkyl imidazolium cation substituents is much less pronounced.

Physicochemical properties

Density

A variety of physicochemical properties of the ILs **2**-**4** were determined and are presented in Table 2. The densities of the RTILs **2a**-**b**, **3a**-**c** and **4a**-**b** were measured at 30 °C. Imidazolium cation-anion interactions and molecular packing are the parameters that determine the density. The anion exerts a strong influence on the density, which decreases in the order $PF_6^- > BF_4^- > H_3CSO_3^-$. This shows that the more bulky PF_6 anion is responsible for a more dense molecular packing. Apparently, the hydrogen bonding strength is not a decisive factor. Other trends are seen for the 1-alkyl ether and 1-alkyl imidazolium cation substituents. Ether-functionalized RTILs with the longer 1-triethylene glycol monomethyl ether substituent are less dense. Furthermore, the 1-alkyl ether functionalized RTIL **3a** has a higher density compared to 1-alkyl functionalized RTIL **3c**. These trends are consistent with previously reported data and enforce that it is possible to fine-tune the density of RTILs by structural modifications in the cation and anion.[12]

Phase transitions

Differential scanning calorimetry experiments were performed to gain information about the phase transitions of the imidazolium salts **2**-**4** and the results are presented in Table 2.

Most of the salts reported herein are RTILs, only the 1-alkyl methanesulfonate salts **2c** and **2d** are solid at room-temperature. The 1-alkyl ether RTILs were obtained as yellow liquids due to a tiny amount of a yellow impurity. Although not further considered in the following discussion, it should be kept in mind that this impurity could affect the phase transitions.[1-3]

Interestingly, only a glass transition was observed for the 1-alkyl ether RTILs **2a**-**b**, **3a**-**b** and **4a**, and 1-alkyl

Table 2. Physicochemical properties of the imidazolium ionic liquids **2**-**4**

IL **2-4**	Cation	Anion	d / (g mL^{-1})[a]	T_g / (°C)[b]	T_c / (°C)[c]	T_m / (°C)[d]	T_d / (°C)[e]
2a	$[C_7O_3MIm]^+$	$[H_3CSO_3]^-$	1.23	-59	-	-	196
2b	$[C_3O_1MIm]^+$	$[H_3CSO_3]^-$	1.26	-56	-	-	250
2c	$[C_{10}MIm]^+$	$[H_3CSO_3]^-$	-[f]	-	-5[g]	32	295
2d	$[C_4MIm]^+$	$[H_3CSO_3]^-$	-[f]	-60	-41	44	n.d.[h]
3a	$[C_7O_3MIm]^+$ $[C_5O_2MIm]^+$	$[BF_4]^-$ $[BF_4]^-$	1.25	-68 (-86)[i]	-	-	266
3b	$[C_3O_1MIm]^+$	$[BF_4]^-$	1.29	-75 (-88)[i]	-	-	252
3c	$[C_{10}MIm]^+$	$[BF_4]^-$	1.07	-35	-32	0	310
3d	$[C_4MIm]^+$	$[BF_4]^-$	n.d.[h]	-86	-	-	n.d.[h]
4a	$[C_7O_3MIm]^+$ $[C_5O_2MIm]^+$	$[PF_6]^-$ $[PF_6]^-$	1.37	-60 (-69)[i]	-	-	184
4b	$[C_3O_1MIm]^+$	$[PF_6]^-$	1.45	-70	-29	10 (15)[i]	156

[a]Density at 30 °C. [b]Glass transition temperature determined by DSC on heating. [c]Crystallization temperature determined by DSC on heating. [d]Melting point determined by DSC on heating. [e]Decomposition temperature determined by TGA. [f]Solid at 30 °C. [g]Crystallization temperature determined by DSC on cooling. [h]Not determined. [i]Reported values in reference 9.

RTIL **3d**.[9,28] In other words, crystallization does not occur upon cooling of these RTILs to low temperatures. This indicates that these RTILs are completely amorphous (0% crystallinity). In contrast, only a crystallization exotherm and melting endotherm were observed for methanesulfonate salt **2c**, which is related to a 100% crystallinity. The ILs **2d**, **3c** and **4b** have both crystalline and amorphous domains as glass transition endotherms as well as crystallization exotherms and melting endotherms were detected. A consistent correlation between crystallinity and structural modifications does not exist for the ILs **2**-**4**. However, a few isolated trends are visible: (*i*) A higher crystallinity is observed when the imidazolium cation is functionalized with a longer 1-alkyl chain (**2c** vs **2d** and **3c** vs **3d**); (*ii*) Crystallinity disappears completely upon substitution of the 1-decyl chain with the 1-triethylene glycol monomethyl ether functionality (**2c** vs **2a** and **3c** vs **3a**), which could be due to the higher rotational freedom of the 1-alkyl ether chain; (*iii*) The 1-alkyl tetrafluoroborate RTILs **3c** and **3d** have lower crystallinities compared to their methanesulfonate equivalents **2c** and **2d**.

One of the most important parameters of ILs is their liquid range. The lower limit of the liquid range is either determined by the glass transition temperature for completely amorphous ILs or by the melting point for ILs with crystallinity. Alfonso and co-workers[9] previously reported the synthesis and phase transitions (Table 2) of the 1-monoethylene glycol monomethyl ether-3-methylimidazolium BF_4 and PF_6 ILs **3b** and **4b**, and the 1-diethylene glycol monomethyl ether-3-methylimidazolium BF_4 and PF_6 ILs. Figure 4 shows the DSC traces of the cation **A** [C_7O_3MIm] based RTILs **2a**, **3a** and **4a**. For all cations **A**-**D** (Figure 1), modification of the anion results in an increase of the solid-liquid transition temperature in the order $BF_4^- < PF_6^- < H_3CSO_3^-$. However, other general trends upon modification of the imidazolium cation are not visible.

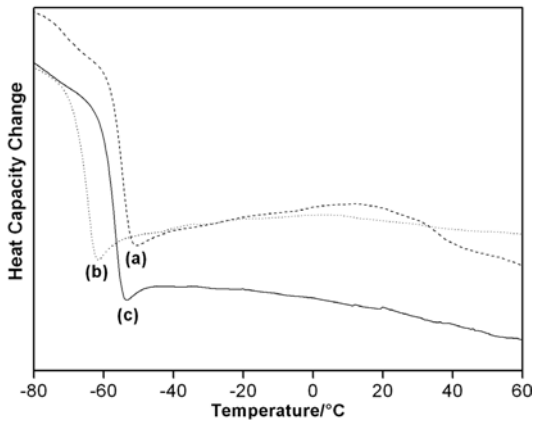

Figure 4. DSC heating traces of the RTILs **2a** $[C_2O_3MIm]^+[H_3CSO_3]^-$ (a), **3a** $[C_7O_3MIm]^+[BF_4]^-$ (b) and **4a** $[C_7O_3MIm]^+[PF_6]^-$ (c).

Decomposition temperature

Thermal gravimetric analysis experiments were used to determine the decomposition temperature (upper limit of the liquid range) of the ILs **2**-**4**. The results are shown in Table 2 and the TGA traces of the RTILs **2b**, **3b** and **4a**-**b** are presented in Figure 5. Interestingly, the BF_4 RTILs have both the highest thermal stability and lowest solid-liquid transition temperatures. Table 3 shows a highly anion dependent thermal stability, which decreases in the order $BF_4^- > H_3CSO_3^- > PF_6^-$. Furthermore, the 1-alkyl ether functionalized RTILs **2a** and **3a** have lower decomposition temperatures in comparison to their 1-alkyl equivalents **2c** and **3c**. Hexafluorophosphate RTIL **4b** has the lowest thermal stability.

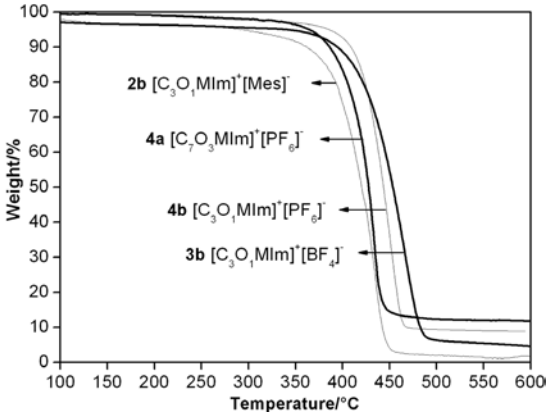

Figure 5. TGA traces of the ILs **2b**, **3b**, **4a** and **4b**.

Conclusions

In summary, a complementary set of 1-alkyl ether and 1-alkyl functionalized imidazolium ILs was successfully prepared via a halide-free approach. Most of these salts are RTILs, but the 1-alkyl methanesulfonate ILs **2c**-**d** are solid at room-temperature. Hydrogen bonding interactions between the aromatic heterocyclic protons and the IL anion are principally anion dependent and decrease in the order $H_3CSO_3^- > BF_4^- > PF_6^-$. In comparison, the acidity of the imidazolium ring H^2 proton is strongly enhanced for the methanesulfonate ILs **2**. The density is easily fine-tuned within this set of RTILs **2**-**4** due to a linear response upon structural modifications: (*i*) $PF_6^- > BF_4^- > H_3CSO_3^-$; (*ii*) $C_3O_1MIm > C_7O_3MIm$; (*iii*) $C_7O_3MIm > C_{10}MIm$. In contrast, physicochemical properties like phase transitions and decomposition temperature are tuneable by structural modifications, but, although some trends are observed, their correlation is less predictive. Almost all 1-alkyl ether functionalized RTILs only have a glass transition and are completely

amorphous materials. Interestingly, the broadest liquid ranges were identified for the tetrafluoroborate RTILs. The lower limit (solid-liquid transition temperature) increases in the order $BF_4^- < PF_6^- < H_3CSO_3^-$. On the other side (upper limit), the tetrafluoroborate RTILs have the highest decomposition temperatures ((1) $BF_4^- > H_3CSO_3^- > PF_6^-$; (2) 1-alkyl > 1-alkyl ether). Altogether, the presented IL characterization study is of importance to obtain a better understanding of their application scope. Besides, this knowledge could facilitate the development of new task-specific ILs.

Acknowledgments

The authors thank the CNPq for financial support. H.S.S. thanks the CNPq for a visiting scientist fellowship.

Supplementary Information

^{1}H and ^{13}C NMR of **1a**, **2a**, **2c**, **3a** and **4a**, and TGA traces of **2a**, **2c**, **3a**, **3c** and **4a**. This material is available free of charge at http://jbcs.sbq.org.br, as pdf file.

References

1. Dupont, J.; Consorti, C. S.; Spencer, J.; *J. Braz. Chem. Soc.* **2000**, *11*, 337.
2. Dupont, J.; de Souza, R. F.; Suarez, P. A. Z.; *Chem. Rev.* **2002**, *102*, 3667.
3. Welton, T.; *Chem. Rev.* **1999**, *99*, 2071.
4. Astruc, D.; Lu, F.; Aranzaes, J. R.; *Angew. Chem.* **2005**, *117*, 8062; *Angew. Chem., Int. Ed.* **2005**, *44*, 7852; Roucoux, A.; Schulz, J.; Patin, H.; *Chem. Rev.* **2002**, *102*, 3757; Ott, L. S.; Finke, R. G.; *Coord. Chem. Rev.* **2007**, *251*, 1075; Migowski, P.; Dupont, J.; *Chem. Eur. J.* **2007**, *13*, 32.
5. Klingshirn, M. A.; Spear, S. K.; Holbrey, J. D.; Rogers, R. D.; *J. Mater. Chem.* **2005**, *15*, 5174; Zhou, Y.; Schattka, J. H.; Antonietti, M.; *Nano Lett.* **2004**, *4*, 477.
6. de Souza, R. F.; Padilha, J. C.; Gonçalves, R. S.; Dupont, J.; *Electrochem. Commun.* **2003**, *5*, 728; Markevich, E.; Baranchugov, V.; Aurbach, D.; *Electrochem. Commun.* **2006**, *8*, 1331; Snook, G. A.; Best, A. S.; Pandolfo, A. G.; Hollenkamp, A. F.; *Electrochem. Commun.* **2006**, *8*, 1405; de Souza, R. F.; Padilha, J. C.; Gonçalves, R. S.; de Souza, M. O.; Rault-Berthelot, J.; *J. Power Sources* **2007**, *164*, 792; Abedin, S. Z. E.; Endres, F.; *Chem. Phys. Chem.* **2006**, *7*, 58.
7. Lee, S. G.; *Chem. Commun.* **2006**, *10*, 1049; Davis, J. H.; *Chem. Lett.* **2004**, *33*, 1072; Fei, Z. F.; Geldbach, T. J.; Zhao, D. B.; Dyson, P. J.; *Chem. Eur. J.* **2006**, *12*, 2122.
8. Donato, R. K.; Migliorini, M. V.; Benvegnú, M. A.; Dupont, J.; Gonçalves, R. S.; Schrekker, H. S.; *J. Solid State Electrochem.* **2007**, *11*, 1481; Schrekker, H. S.; Gelesky, M. A.; Stracke, M. P.; Schrekker, C. M. L.; Machado, G.; Teixeira, S. R.; Rubim, J. C.; Dupont J.; *J. Colloid Interface Sci.* **2007**, *316*, 189; Schrekker, H. S.; Stracke, M. P.; Schrekker, C. M. L.; Dupont, J.; *Ind. Eng. Chem. Res.* **2007**, *46*, 7389.
9. Branco, L. C.; Rosa, J. N.; Ramos, J. J. M.; Afonso, C. A. M.; *Chem. Eur. J.* **2002**, *8*, 3671.
10. Bonhôte, P.; Dias, A-P.; Papageorgiou, N.; Kalyanasundaram, K.; Grätzel, M.; *Inorg. Chem.* **1996**, *35*, 1168; Dzyuba, S. V.; Bartsch, R. A.; *Tetrahedron Lett.* **2002**, *43*, 4657; Ramos, J. J. M.; Afonso, C. A. M.; Branco, L. C.; *J. Therm. Anal. Calorim.* **2003**, *71*, 659; Liu, H.; Wang, H-Z.; Tao, G-H.; Kou, Y.; *Chem. Lett.* **2005**, *34*, 1184; Dzyuba, S. V.; Bartsch, R. A.; *Tetrahedron Lett.* **2002**, *43*, 4657.
11. Cassol, C. C.; Ebeling, G.; Ferrera, B.; Dupont, J.; *Adv. Synth. Catal.* **2006**, *348*, 243.
12. Zhou, Z-B.; Matsumoto, H.; Tatsumi, K.; *Chem. Eur. J.* **2004**, *10*, 6581.
13. Ishida, Y.; Sasaki, D.; Miyauchi, H.; Saigo, K.; *Tetrahedron Lett.* **2004**, *45*, 9455.
14. Valente, A. A.; Petrovski, Ž.; Branco, L. C.; Afonso, C. A. M.; Pillinger, M.; Lopes, A. D.; Romão, C. C.; Nunes, C. D.; Gonçalves, I. S.; *J. Mol. Catal. A: Chem.* **2004**, *218*, 5; Mehdi, H.; Bodor, A.; Lantos, D.; Horváth, I. T.; De Vos, D. E.; Binnemans, K.; *J. Org. Chem.* **2007**, *72*, 517; Branco, L. C.; Afonso, C. A. M.; *J. Org. Chem.* **2004**, *69*, 4381; Wang, L.; Zhang, Y.; Xie, C.; Wang, Y.; *Synlett* **2005**, *12*, 1861.
15. Park, S.; Viklund, F.; Hult, K.; Kazlauskas, R. J.; *Green Chem.* **2003**, *5*, 715; Kim, M-J.; Choi, M. Y.; Lee, J. K.; Ahn, Y.; *J. Mol. Catal. B: Enzym.* **2003**, *26*, 115; Park, S.; Kazlauskas, R. J.; *J. Org. Chem.* **2001**, *66*, 8395.
16. Prasad, A. K.; Kumar, V.; Malhotra, S.; Ravikumar, V. T.; Sanghvi, Y. S.; Parmar, V. S.; *Bioorg. Med. Chem.* **2005**, *13*, 4467; Kimizuka, N.; Nakashima, T.; *Langmuir* **2001**, *17*, 6759; Uzagare, M. C.; Sanghvi, Y. S.; Salunkhe, M. M.; *Green Chem.* **2003**, *5*, 370.
17. Pernak, J.; Sobaszkiewicz, K.; Mirska, I.; *Green Chem.* **2003**, *5*, 52.
18. Luo, H.; Dai, S.; Bonnesen, P. V.; Buchanan III, A. C.; *J. Alloys Compd.* **2006**, *418*, 195; Holbrey, J. D.; Visser, A. E.; Spear, S. K.; Reichert, W. M.; Swatloski, R. P.; Broker, G. A.; Rogers, R. D.; *Green Chem.* **2003**, *5*, 129.
19. Fraga-Dubreuil, J.; Famelart, M-H.; Bazureau, J. P.; *Org. Process Res. Dev.* **2002**, *6*, 374.
20. Pernak, J.; Czepukowicz, A.; Pozniak, R.; *Ind. Eng. Chem. Res.* **2001**, *40*, 2379.
21. Wang, Z.; Wang, Q.; Zhang, Y.; Bao, W.; *Tetrahedron Lett.* **2005**, *46*, 4657.
22. Yoshio, M.; Mukai, T.; Ohno, H.; Kato, T.; *J. Am. Chem. Soc.* **2004**, *126*, 994.
23. Jin, C. M.; Ye, C. F.; Phillips, B. S.; Zabinski, J. S.; Liu, X. Q.; Liu, W. M.; Shreeve, J. M.; *J. Mater. Chem.* **2006**, *16*, 1529.

24. Lange, N. A.; *Lange´s Handbook of Chemistry,* Dean, J. A., ed.; 11th ed., McGraw-Hill Professional Publishing: McGraw-Hill, 1973.
25. Dupont, J.; Suarez, P. A. Z.; *Phys. Chem. Chem. Phys.* **2006**, *8*, 2441; Gozzo, F. C.; Santos, L. S.; Augusti, R.; Consorti, C. S.; Dupont, J.; Eberlin, M. N.; *Chem. Eur. J.* **2004**, *10*, 6187.
26. Suarez, P. A. Z.; Einloft, S.; Dullius, J. E. L.; de Souza, R. F. ; Dupont, J.; *J. Chim. Phys.* **1998**, *95*, 1626.
27. van den Broeke, J. ; Stam, M.; Lutz, M.; Kooijman, H.; Spek, A. L.; Deelman, B-J.; van Koten, G.; *Eur. J. Inorg. Chem.* **2003**, 2798.
28. Headley, A. D.; Jackson, N. M.; *J. Phys. Org. Chem.* **2002**, *15*, 52.
29. Wang, Y.; Li, H.; Han, S.; *J. Chem. Phys.* **2006**, *124*, 044504; Dong, K.; Zhang, S.; Wang, D.; Yao, X.; *J. Phys. Chem. A* **2006**, *110*, 9775; Hanke, C. G.; Atamas, N. A.; Lynden-Bell, R. M.; *Green Chem.* **2002**, *4*, 107.

Received: August 28, 2007
Web Release Date: February 20, 2008

J. Braz. Chem. Soc., Vol. 13, No. 3, S1-S8, 2008.
Printed in Brazil - ©2008 Sociedade Brasileira de Química
0103 - 5053 $6.00+0.00

Preparation, Cation-Anion Interactions and Physicochemical Properties of Ether-Functionalized Imidazolium Ionic Liquids

Henri S. Schrekker,* Dagoberto O. Silva, Marcos A. Gelesky, Marcelo P. Stracke, Clarissa M. L. Schrekker, Reinaldo S. Gonçalves and Jairton Dupont*

Instituto de Química, Universidade Federal do Rio Grande do Sul, Av. Bento Gonçalves, 9500, CP 15003, 91501-970 Porto Alegre-RS, Brazil

Experimental

General

All reactions were carried out under an argon atmosphere in dried glassware using standard Schlenk, syringe and septa techniques. ^{1}H and ^{13}C NMR spectra were recorded on a Varian Inova 300 MHz spectrometer in $CDCl_3$ or d6-acetone. Chemical shifts are reported relative to TMS in $CDCl_3$ (δ 0.00 for ^{1}H), residual d5-acetone (δ 2.05 for ^{1}H), $CDCl_3$ (δ 77.00 for ^{13}C), and d6-acetone (δ 30.5 for ^{13}C). Chemical shifts δ are quoted in parts per million (ppm), and coupling constants *J* are given in hertz (Hz). IR-spectra were recorded in a range of 4000-500 cm^{-1} using a Shimadzu FTIR-8300 Fourier Transform Infrared Spectrophotometer, and were measured as neat oil or as film (w = weak, m = medium, and s = strong). Mass spectra were recorded on a Waters Micromass Q-Tof micro quadrapole mass spectrometer in ESI-mode.

Materials

The solvents dichloromethane, acetone and diethyl ether were purchased from VETEC Química Fina LTDA and used without further purification. Triethylene glycol monomethyl ether, 2-methoxyethanol, 1-decanol, 1-butanol, methanesulfonic acid, sodium tetrafluoroborate and potassium hexafluorophosphate were used as purchased from Sigma-Aldrich. The reagents triethylamine, methanesulfonyl chloride and 1-methylimidazole were purchased from Sigma-Aldrich and distilled under argon prior to use. $CDCl_3$ and d6-acetone were purchased from Cambridge Isotope Laboratories. Activated carbon, celite, basic aluminum oxide and silica gel 60 (40-60 μm) were purchased from Merck. A procedure reported previously in the literature was used for the synthesis of **1d**,[1] **2d**[1] and **3d**,[1] and the spectral data were in accordance with the literature data.

*General procedure for the synthesis of alkylating agents **1a-c***

A modified literature procedure was used for the synthesis of **1a**-**c**.[1] Alcohol (1.00 equiv.), methanesulfonyl chloride (1.05 equiv.), triethylamine (1.10 equiv.) and dichloromethane. Alkylating agents **1a** and **1c** were not purified by a vacuum distillation as decomposition occurred at elevated temperatures. Instead of this, **1a** and **1c** were dissolved in dichloromethane and treated with activated carbon. Filtration over a short silica column, solvent evaporation, and vacuum drying at 70 °C for 8 hours resulted in the isolation of **1a** as a yellow liquid and **1c** as a colorless liquid. Alkylating agent **1b** was obtained as a colorless liquid after vacuum distillation. The alkylating agents **1a**-**c** were obtained in high yields (>90 %). Spectral data of **1b**[2] and **1c**[3] were in agreement with those previously reported in the literature.

*General procedure for the synthesis of methanesulfonate ILs **2a-c***

A modified literature procedure was used for the synthesis of **2a**-**c**.[1] The mixture of **1a**-**c** (1.000 equiv.) and 1-methylimidazole (1.001 equiv.) was heated at 60 °C for 24 hours. ILs **2a**-**b** were dissolved in dichloromethane. Methanesulfonic acid was added in order to remove excess 1-methylimidazole and the reaction mixture was stirred for 15 minutes at 25 °C. Filtration over a short basic aluminum/celite column was followed by the removal of the dichloromethane. Consecutively, **2a** and **2b** were dissolved in acetone and treated with activated carbon. Filtration over a short celite column, solvent evaporation, and vacuum dry-

*e-mail: schrekker@iq.ufrgs.br ; dupont@iq.ufrgs.br

ing at 100-120 °C for 8 hours resulted in the isolation of **2a** and **2b** as yellow liquids. Room-temperature ionic salt **2c** was dissolved in hot acetone. White crystals of **2c** formed upon cooling, and diethyl ether was added to promote the crystallization. Ionic salt **2c** was vacuum dried at 30 °C for 8 hours. The very hygroscopic ILs **2a**-**c** were obtained in high yields (>90 %). Cyclic voltammetry experiments indicated the absence of a significant amount of water in the ILs. Spectral data of **2b**[4] were in agreement with those previously reported in the literature.

*General procedure for the synthesis of tetrafluoroborate ILs **3a-c** and hexafluorophosphate ILs **4a**-**b***

A modified literature procedure was used for the synthesis of **3a**-**c** and **4a**-**b**.[5] $NaBF_4$ (1.12 equiv.) or KPF_6 (1.12 equiv.) were added to a solution of IL **2a**-**c** (1.0 equiv.) in acetone at 25 °C. The NaO_3SCH_3 and KO_3SCH_3 salts were removed by filtration after 2 hours at 25 °C. Activated carbon was added to the acetone solution and the reaction mixture was stirred for 24 hours at 25 °C. Removal of the activated carbon by filtration was followed by the removal of the acetone. Consecutively, the ILs were dissolved in dichloromethane. Filtration over a short celite column, solvent evaporation and vacuum drying at 100-120 °C (**3a**-**c** and **4a**) or 75 °C (**4b**) for 8 hours resulted in the isolation of **3a**-**c** and **4a**-**b** in high yields (>90 %). The ILs **3a**-**b** and **4a**-**b** were isolated as yellow liquids and ionic liquid **3c** as a colorless liquid. Cyclic voltammetry experiments indicated the absence of a significant amount of water in the ILs. Spectral data of **3b**-**c**[5] and **4b**[5] were in agreement with those previously reported in the literature.

References

1. Cassol, C. C.; Ebeling, G.; Ferrera, B.; Dupont, J.; *Adv. Synth. Catal.* **2006**, *348*, 243.
2. Tavecchia, P.; Gentili, P.; Kurz, M.; Sottani, C.; Bonfichi, R.; Selva, E.; Lociuro, S.; Rostelli, E.; Ciabatti, R.; *Tetrahedron* **1995**, *51*, 4867.
3. Ahmed, S.; Owen, C. P.; James, K.; Patel, C. K.; Sampson, L.; *J. Steroid Biochem. Mol. Biol.* **2002**, *80*, 429.
4. Uzagare, M. C.; Sanghvi, Y. S.; Salunkhe, M. M.; *Green Chem.* **2003**, *5*, 370.
5. Branco, L. C.; Rosa, J. N.; Ramos, J. J. M.; Afonso, C. A. M.; *Chem. Eur. J.* **2002**, *8,* 3671.

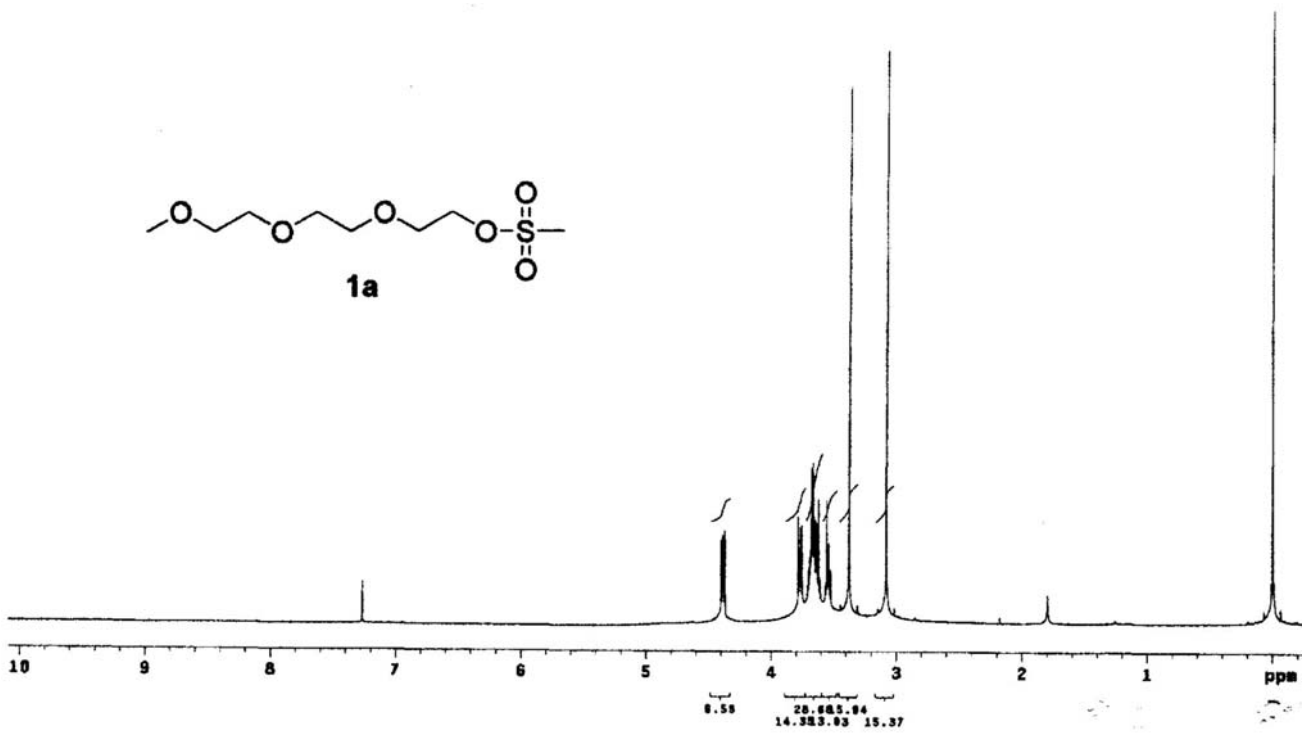

Figure S1. ^{1}H NMR spectrum of compound **1a** (300 MHz, $CDCl_3$).

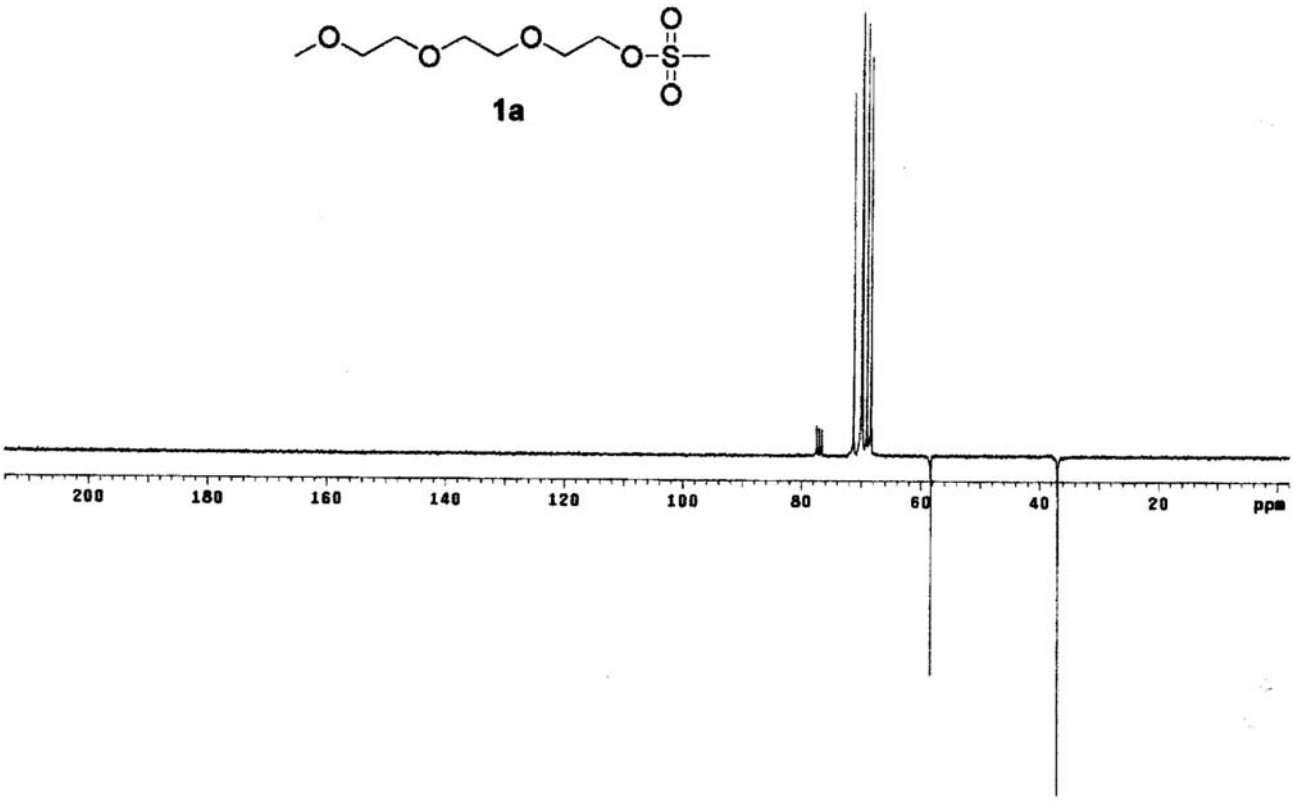

Figure S2. ^{13}C NMR spectrum of compound **1a** (75 MHz, $CDCl_3$).

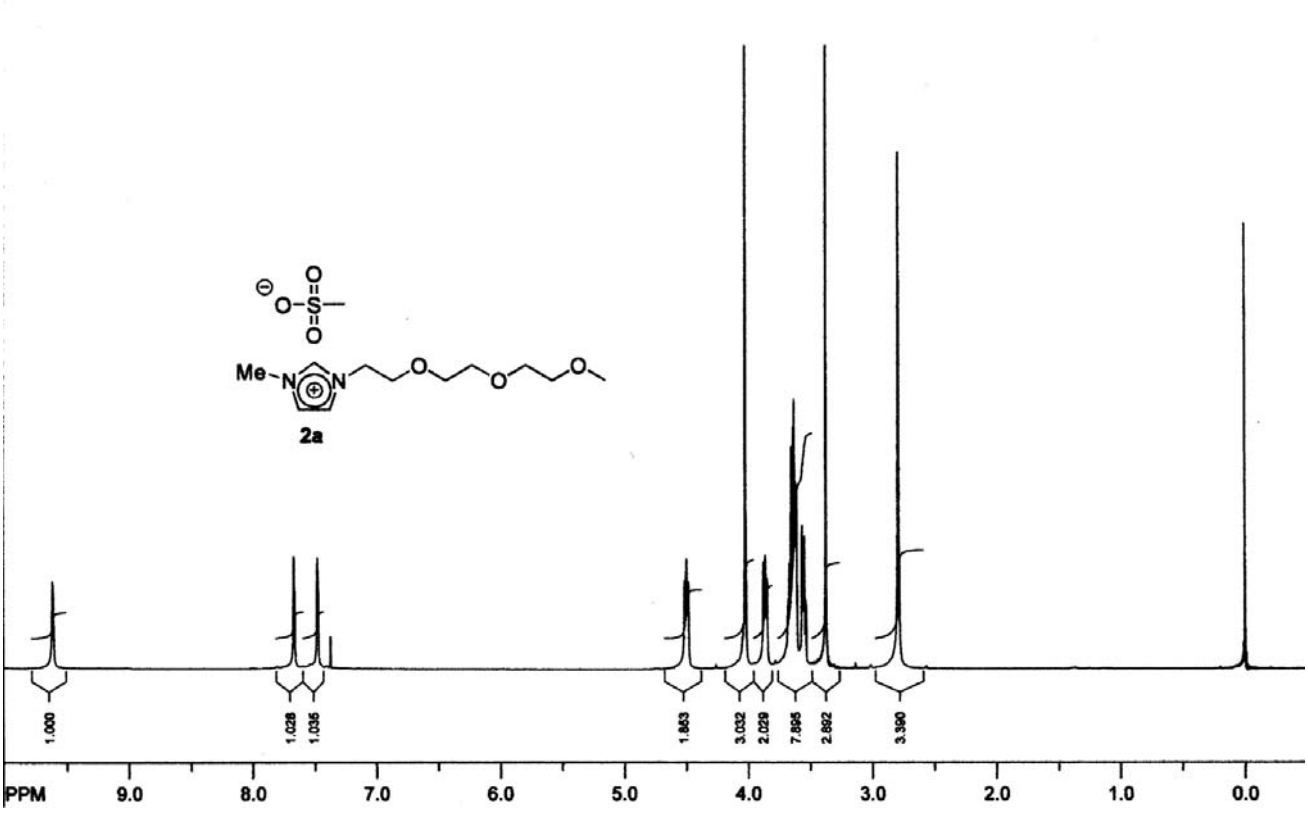

Figure S3. ^{1}H NMR spectrum of ionic liquid **2a** (300 MHz, $CDCl_3$).

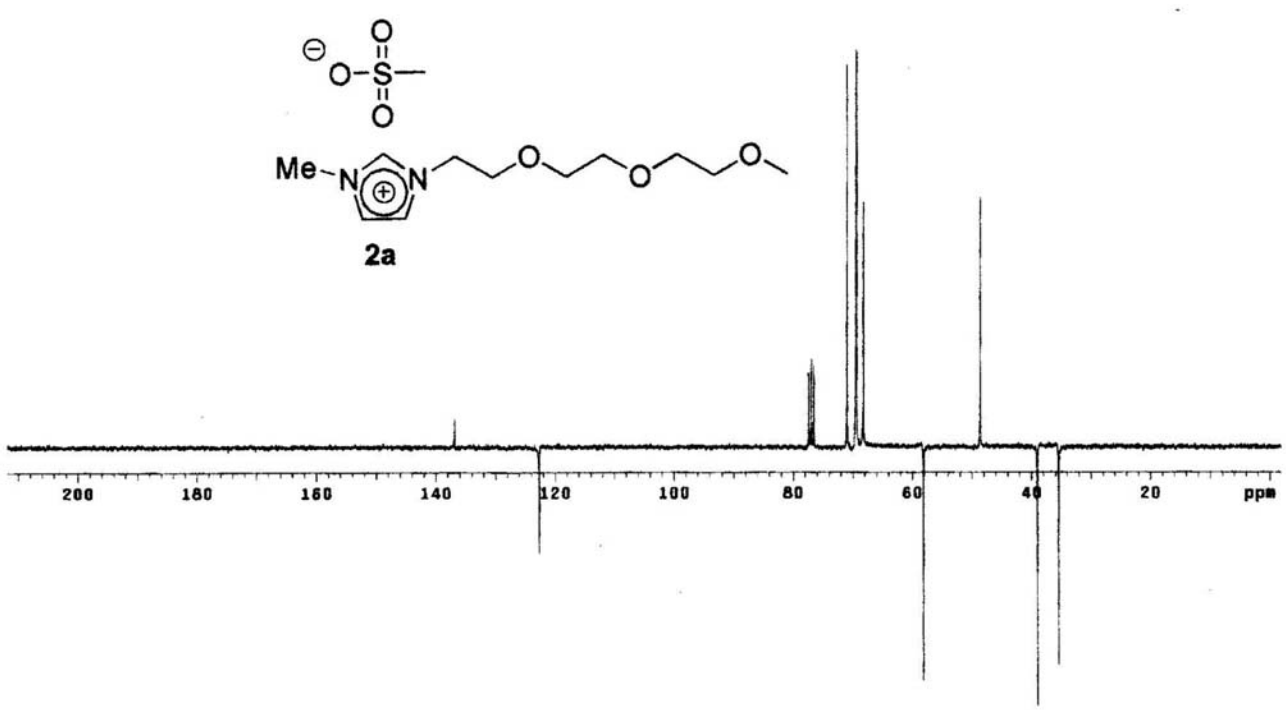

Figure S4. ^{13}C NMR spectrum of ionic liquid **2a** (75 MHz, $CDCl_3$).

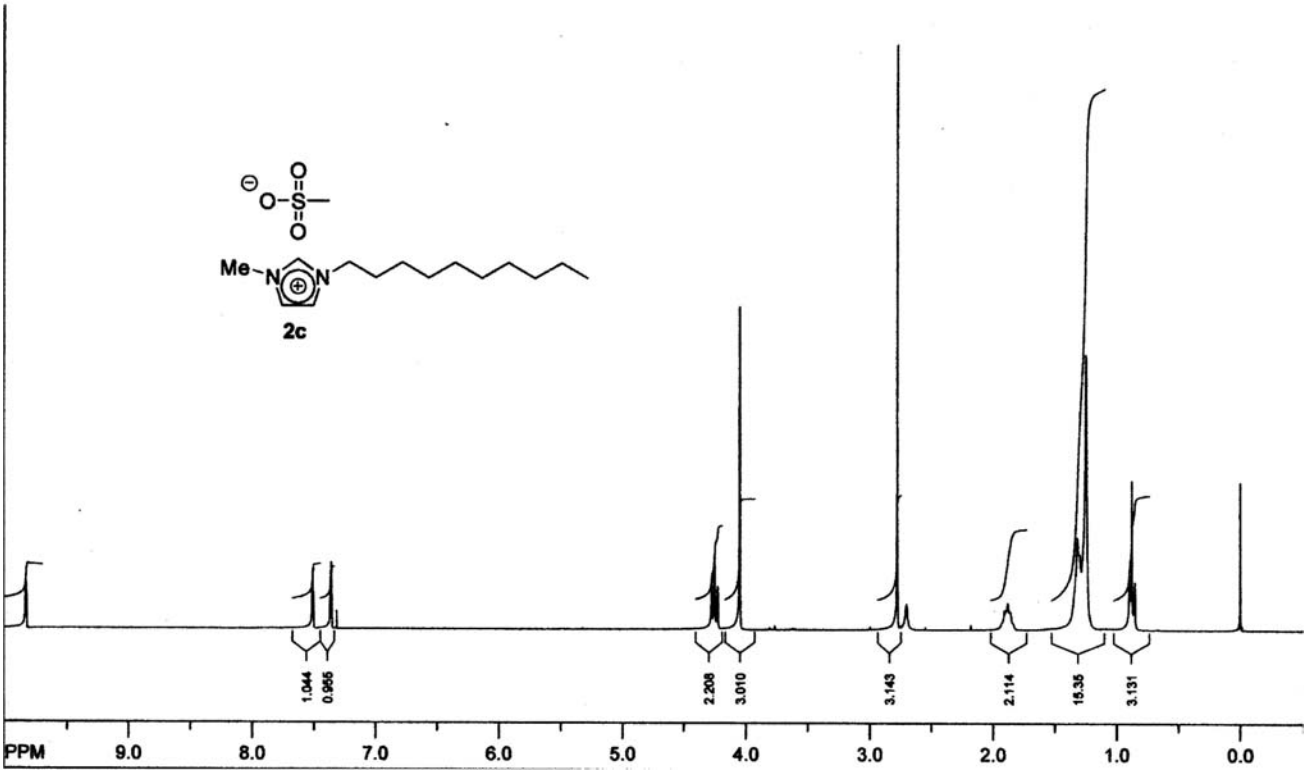

Figure S5. [1]H NMR spectrum of ionic liquid **2c** (300 MHz, $CDCl_3$).

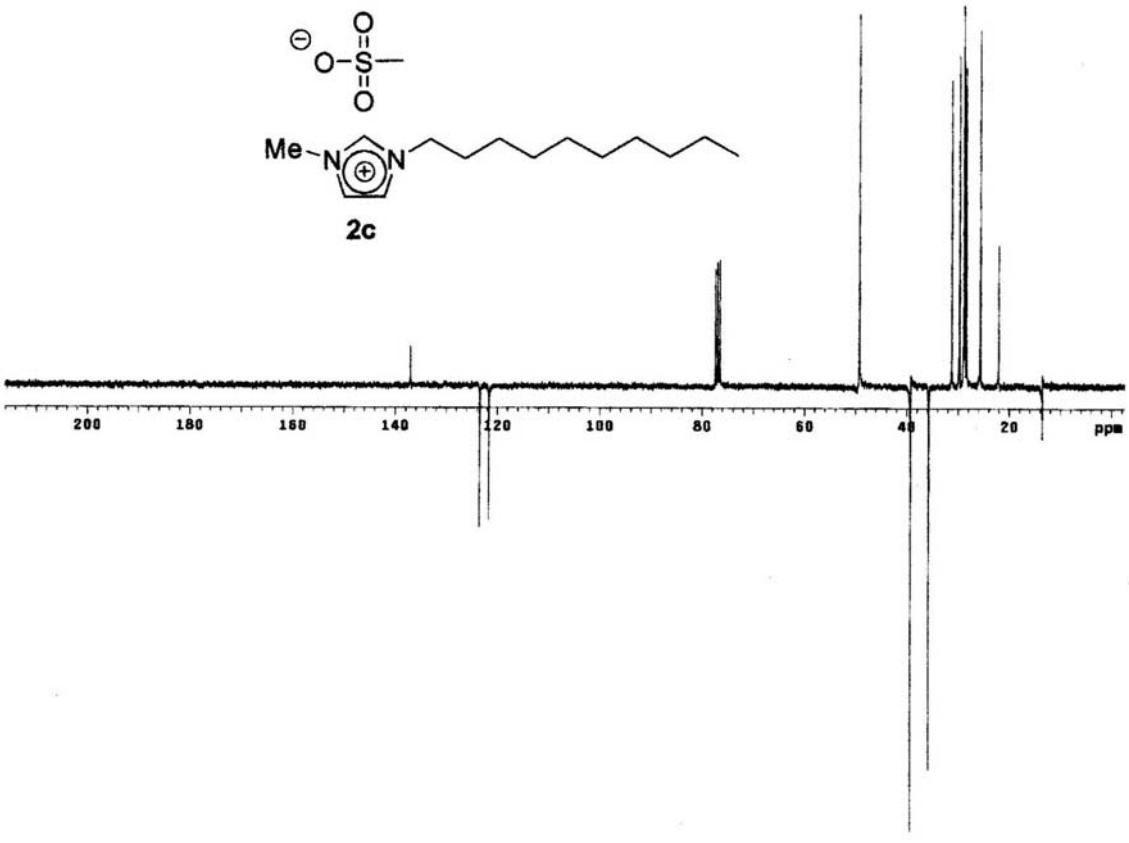

Figure S6. [13]C NMR spectrum of ionic liquid **2c** (75 MHz, $CDCl_3$).

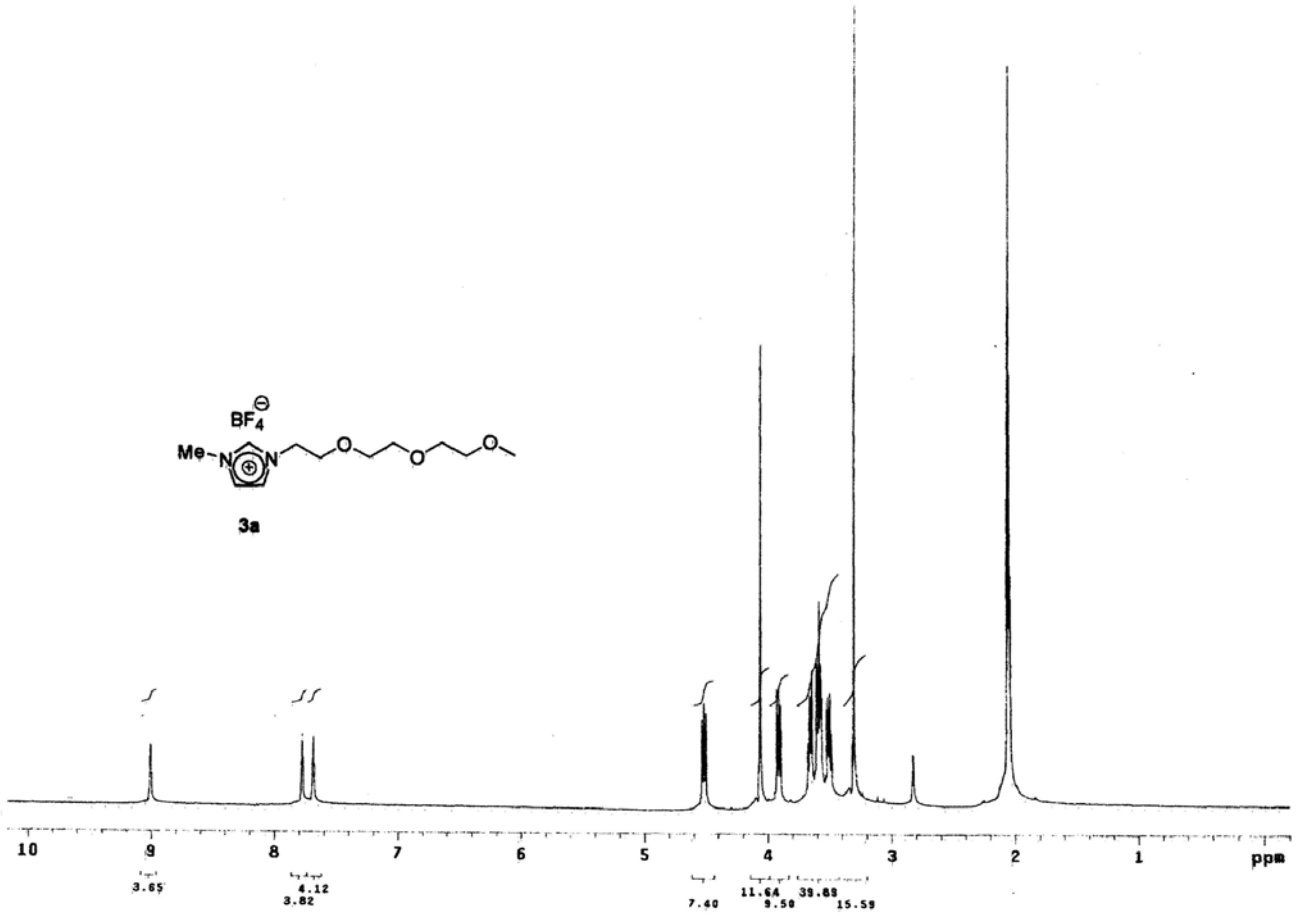

Figure S7. [1]H NMR spectrum of ionic liquid **3a** (300 MHz, d6-acetone).

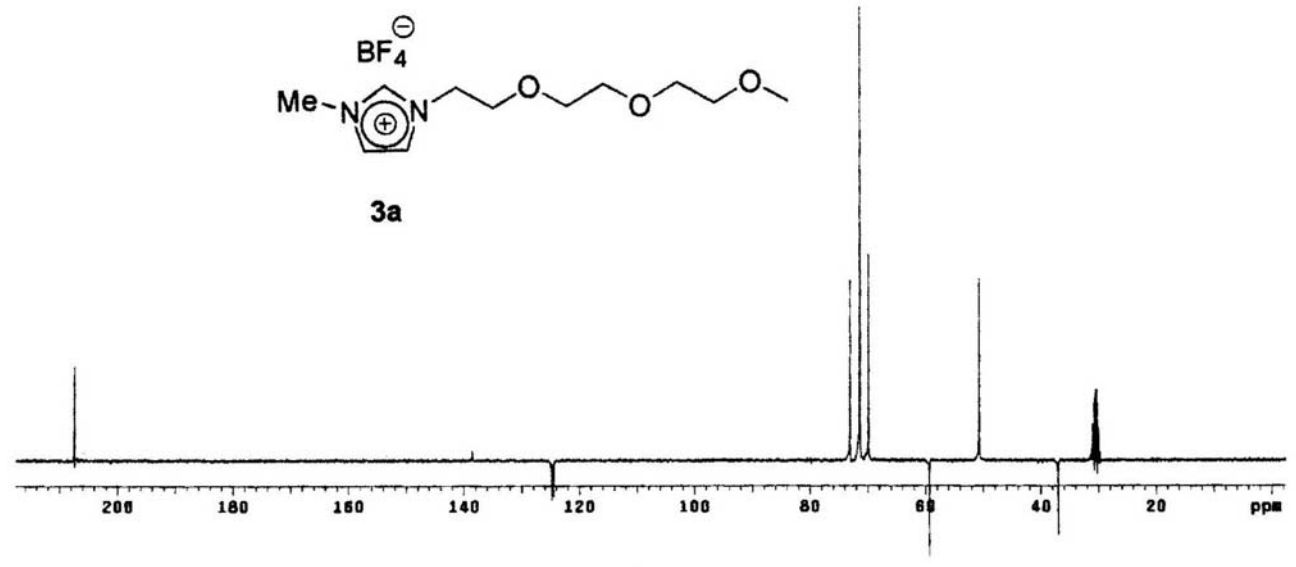

Figure S8. [13]C NMR spectrum of ionic liquid **3a** (75 MHz, d6-acetone).

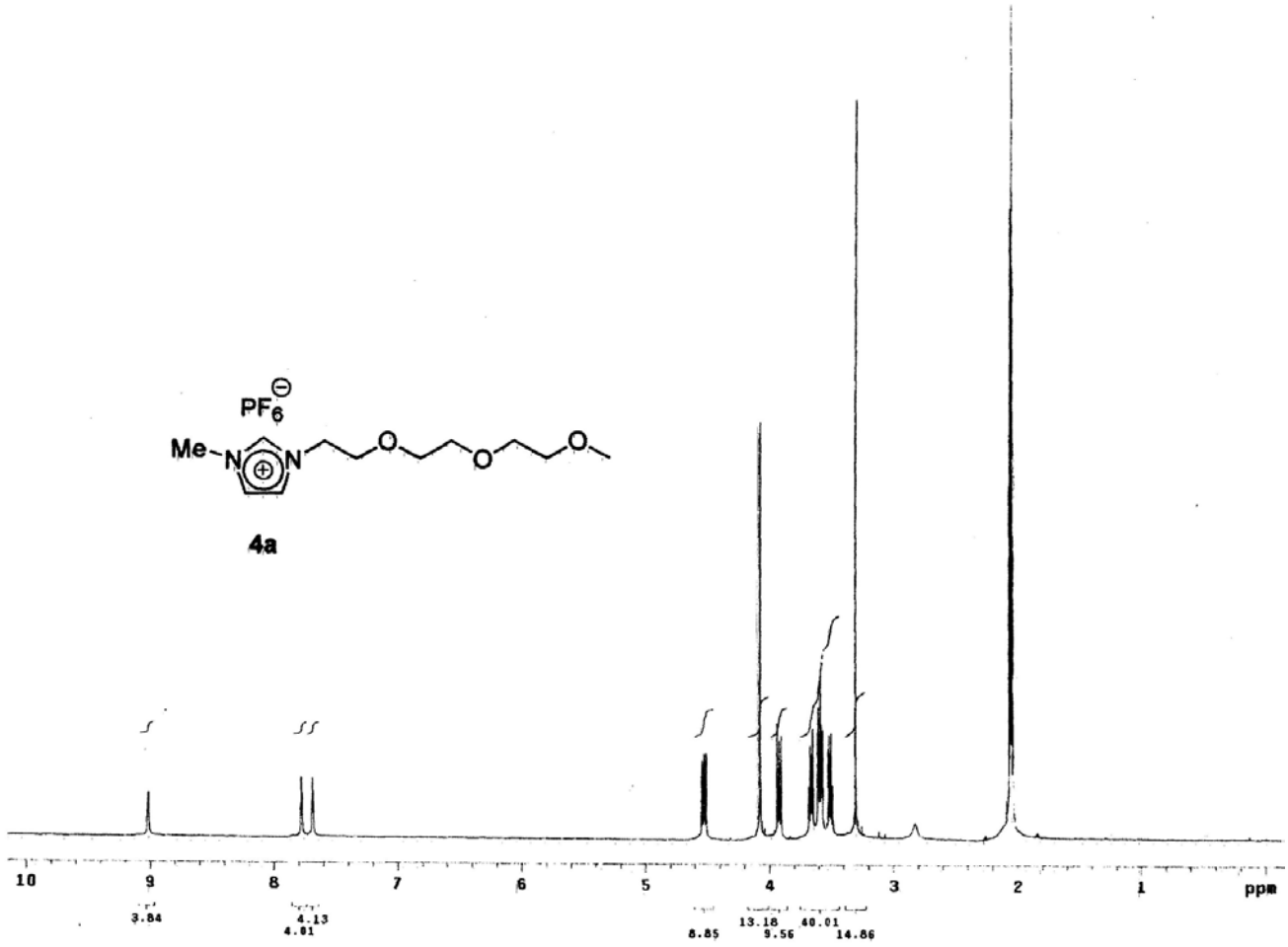

Figure S9. [1]H NMR spectrum of ionic liquid **4a** (300 MHz, d6-acetone).

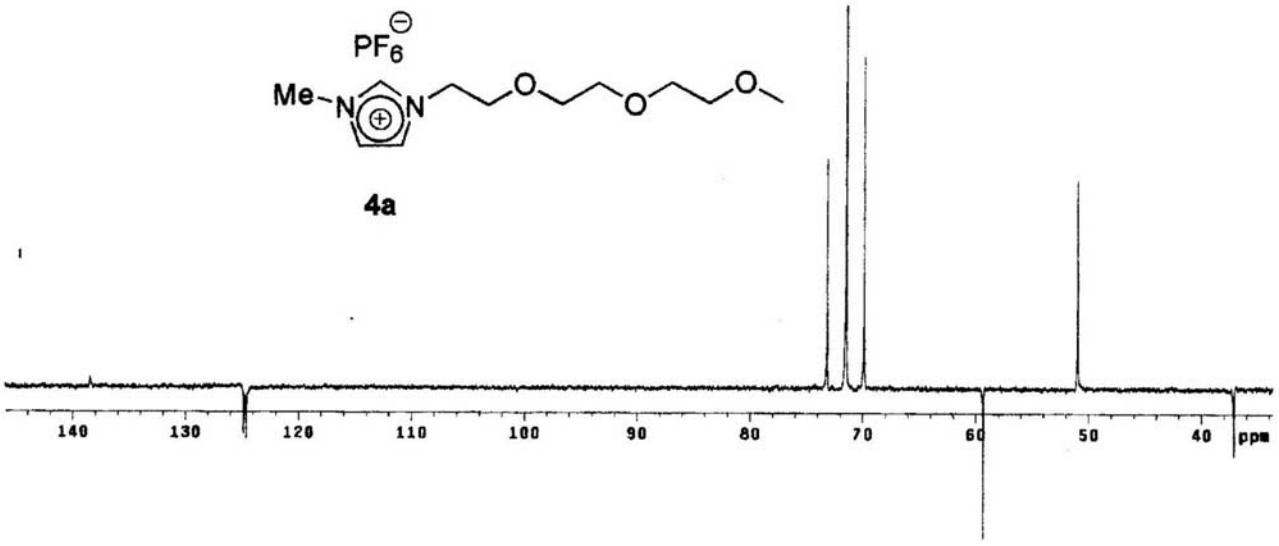

Figure S10. [13]C NMR spectrum of ionic liquid **4a** (75 MHz, d6-acetone).

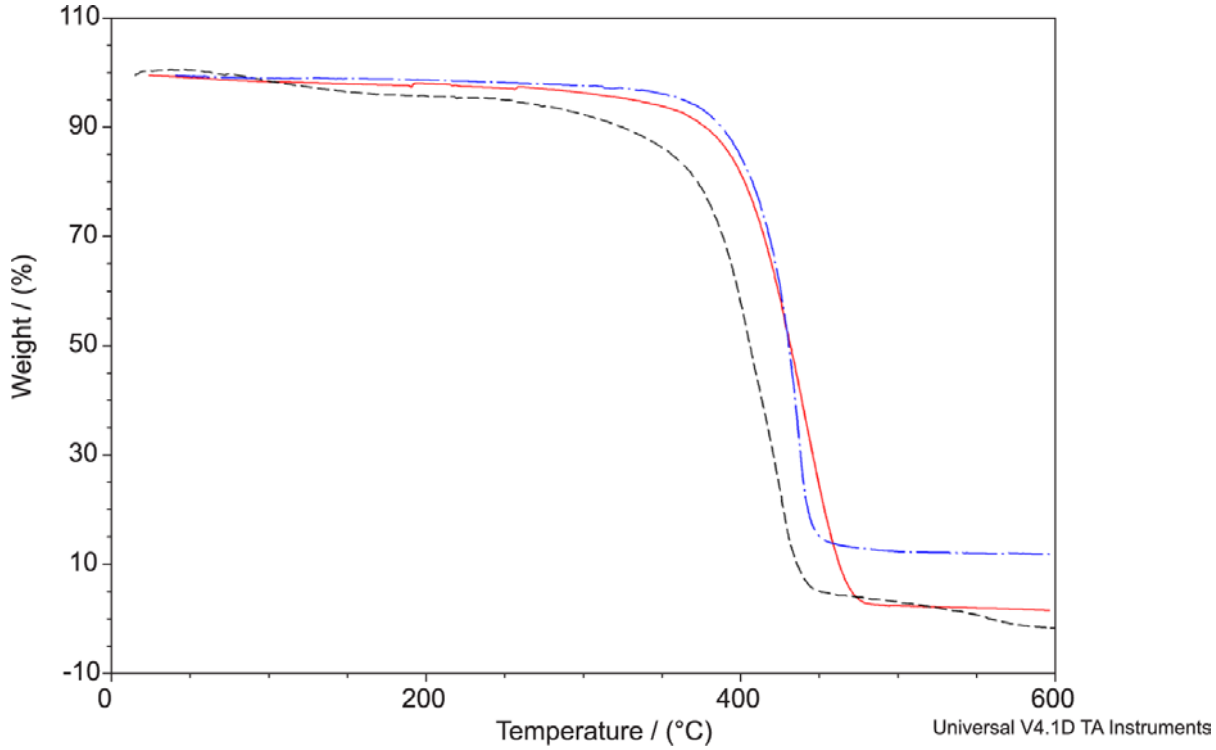

Figure S11. TGA traces of ionic liquid **2a** $[C_7O_3MIm]^+[Mes]^-$ (black line), ionic liquid **3a** $[C_7O_3MIm]^+[BF_4]^-$ (red line) and ionic liquid **4a** $[C_7O_3MIm]^+[PF_6]^-$ (blue line).

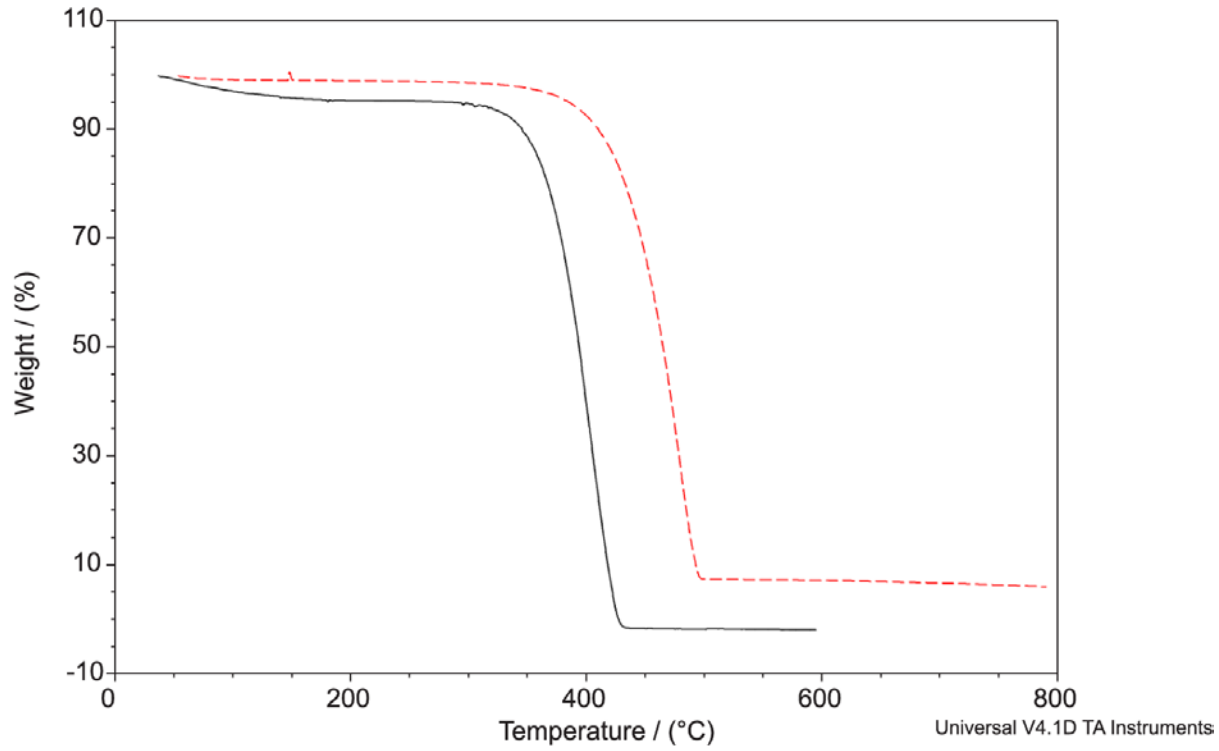

Figure S12. TGA traces of ionic liquid **2c** $[C_{10}MIm]^+[Mes]^-$ (black line) and ionic liquid **3c** $[C_{10}MIm]^+[BF_4]^-$ (red line).